Author Manuscript

Author Manuscript

Author Manuscript

Author Manuscript

HHS Public Access

Author manuscript

Sci Transl Med. Author manuscript; available in PMC 2019 September 04.

Published in final edited form as:

Sci Transl Med. 2019 May 08; 11(491): . doi:10.1126/scitranslmed.aau8587.

HBEGF+ macrophages in rheumatoid arthritis induce fibroblast invasiveness

David Kuo[1,2,*], **Jennifer Ding**[3,†,*], **Ian S. Cohn**[3,‡], **Fan Zhang**[4,5,6,7], **Kevin Wei**[8], **Deepak A. Rao**[8], **Cristina Rozo**[3], **Upneet K. Sokhi**[3], **Sara Shanaj**[3], **David J. Oliver**[3], **Adriana P. Echeverria**[3], **Edward F. DiCarlo**[9], **Michael B. Brenner**[8], **Vivian P. Bykerk**[3,10], **Susan M. Goodman**[3,10], **Soumya Raychaudhuri**[4,5,6,11], **Gunnar Rätsch**[12,2], **Lionel B. Ivashkiv**[3,10,13,§], **Laura T. Donlin**[3,10,§,‖]

[1]Graduate Program in Physiology, Biophysics and Systems Biology, Weill Cornell Graduate School of Medical Sciences, New York, NY 10065, USA. [2]Computational Biology Program, Sloan Kettering Institute, 1275 York Avenue, New York, NY 10065, USA. [3]Arthritis and Tissue Degeneration Program and the David Z. Rosensweig Genomics Research Center, Hospital for

‖ Corresponding author. donlinl@hss.edu.
†Present address: Department of Neurobiology, University of Chicago, Chicago, IL 60637, USA.
‡Present address: Perelman School of Medicine, University of Pennsylvania, Philadelphia, PA 19104, USA.
*Co-first authors.
§Co-senior authors.

Author contributions:

D.K. analyzed sequencing data, prepared figures, and edited the manuscript; J.D. performed experiments and analyzed data; I.S.C. performed experiments and prepared figures; F.Z. analyzed AMP sequencing data and advised on incorporating it into this manuscript; K.W. and D.A.R. designed experimental pipelines and performed experiments; U.K.S., C.R., and S.S. performed experiments; D.J.O. and A.P.E. analyzed sequencing data; AMP recruited patients and performed experiments; E.F.D. scored histology slides; M.B.B. designed and supervised the AMP experimental pipeline; V.P.B. and S.M.G. collected clinical data and samples; S.R. supervised analysis of AMP sequencing data and incorporated it into this manuscript; G.R. supervised analysis of the in vitro and ex vivo sequencing data; L.B.I. jointly conceived the project, oversaw the in vitro coculture experiments, acquired funding, and edited the manuscript; L.T.D. jointly conceived the project, acquired funding, oversaw the in vitro coculture and RA tissue ex vivo assays, wrote the manuscript, and supervised the research experiments and analyses.

SUPPLEMENTARY MATERIALS

stm.sciencemag.org/cgi/content/full/11/491/eaau8587/DC1

Materials and Methods

Fig. S1. Genes defining the CD14+ single-cell clusters and variance across patient samples.

Fig. S2. Identification of synovial HBEGF+ inflammatory macrophages in an independent RA patient study.

Fig. S3. Synovial fibroblasts down-regulate several pathways in TNF-induced macrophages and impose a transcriptome consistent with TNF and prostaglandin exposure.

Fig. S4. Synovial fibroblasts express EGF receptors whereas HBEGF+ inflammatory macrophages express two EGF ligands.

Fig. S5. Synovial fibroblast exposure modifies how RA medications affect TNF-induced macrophages.

Table S1. Patient characteristics for CD14+ synovial single-cell samples.

Table S2. Patient characteristics for CD14+ synovial bulk-sorted samples.

Table S3. RA patient characteristics for the ex vivo synovial tissue assay.

Table S4. Individual patient disease diagnosis, serology, and histology for the ex vivo synovial tissue assay.

Data file S1. Individual subject-level data.

Competing interests:

M.B.B. serves on a scientific advisory board for GlaxoSmithKline and receives royalties from Roche. D.K. is an employee of Juno Therapeutics, a Celgene Company. The other authors declare that they have no competing interests to declare.

Data and materials availability:

The CD14+ synovial single-cell data generated by the AMP consortium is housed at www.immport.org with the study accession number SDY998. RA patient ex vivo synovial cell and fibroblast cell line RNA-seq data have been deposited to the database of Phenotypes and Genotypes with accession numbers phs001340.v1.p1 and phs001529.v1.p1. In vitro coculture RNA-seq data have been deposited in the Gene Expression Omnibus database with accession numbers GSE57723, GSE95588, and GSE100382. All materials and data transferred between HSS and AMP sites were covered under material transfer agreements.

Author Manuscript Author Manuscript Author Manuscript Author Manuscript

Special Surgery, New York, NY 10021, USA. [4]Center for Data Sciences, Brigham and Women's Hospital, Boston, MA 02115, USA. [5]Division of Rheumatology and Genetics, Department of Medicine, Brigham and Women's Hospital, Boston, MA 02115, USA. [6]Department of Biomedical Informatics, Harvard Medical School, Boston, MA 02115, USA. [7]Medical and Population Genetics, Broad Institute of MIT and Harvard, Cambridge, MA 02142, USA. [8]Division of Rheumatology, Immunology, Allergy, Brigham and Women's Hospital and Harvard Medical School, Boston, MA 02115, USA. [9]Department of Pathology and Laboratory Medicine, Hospital for Special Surgery, New York, NY 10021, USA. [10]Weill Cornell Medical College, New York, NY 10021, USA. [11]Arthritis Research UK Centre for Genetics and Genomics, Centre for Musculoskeletal Research, Manchester Academic Health Science Centre, University of Manchester, Oxford Road, Manchester, UK. [12]Department of Computer Science, Universitätstrasse 6, ETH Zürich, 8092 Zürich, Switzerland [13]Weill Cornell Graduate School of Medical Sciences, New York, NY 10021, USA.

Macrophages tailor their function according to the signals found in tissue microenvironments, assuming a wide spectrum of phenotypes. A detailed understanding of macrophage phenotypes in human tissues is limited. Using single-cell RNA sequencing, we defined distinct macrophage subsets in the joints of patients with the autoimmune disease rheumatoid arthritis (RA), which affects ~1% of the population. The subset we refer to as HBEGF$^+$ inflammatory macrophages is enriched in RA tissues and is shaped by resident fibroblasts and the cytokine tumor necrosis factor (TNF). These macrophages promoted fibroblast invasiveness in an epidermal growth factor receptor– dependent manner, indicating that intercellular cross-talk in this inflamed setting reshapes both cell types and contributes to fibroblast-mediated joint destruction. In an ex vivo synovial tissue assay, most medications used to treat RA patients targeted HBEGF$^+$ inflammatory macrophages; however, in some cases, medication redirected them into a state that is not expected to resolve inflammation. These data highlight how advances in our understanding of chronically inflamed human tissues and the effects of medications therein can be achieved by studies on local macrophage phenotypes and intercellular interactions.

INTRODUCTION

Macrophage plasticity provides tailored homeostatic, immunologic, and reparative mechanisms in a wide range of tissues (1, 2). Their transcriptional, epigenetic, and functional versatility allow macrophages to conform to tissue- and disease-specific factors, resulting in phenotypes indicative of the type of tissue and physiologic state (3–9). Macrophages are a unifying feature in chronic human diseases such as atherosclerosis, autoimmunity, and granulomas (2, 10, 11); however, little is known about macrophage phenotypes in the context of human tissue pathology—particularly at single-cell resolution. Furthermore, although in vitro studies have provided valuable insights into the range of macrophage polarization states (12, 13), the relevance of these well-characterized responses has been difficult to document in human tissues.

Author Manuscript Author Manuscript Author Manuscript Author Manuscript

A precise understanding of human tissue macrophages may enable more effective therapeutic decisions for inflammatory diseases, for which it has often been difficult to discern which molecular pathway to target. For example, interleukin-17 (IL-17) and interferon-γ (IFN-γ) have been implicated in the patho-physiology of inflammatory bowel disease, yet blockade of these factors has produced variable results and, in some cases, worsens disease activity, whereas anti–tumor necrosis factor (TNF) therapies are commonly effective (14). Nonsteroidal anti-inflammatory drugs (NSAIDs) treat pain and components of inflammation in the autoimmune disease rheumatoid arthritis (RA), but for unclear reasons, NSAIDs do not curb joint erosion (15), whereas anti-TNF therapies have proven highly effective on both fronts. Macrophages are innate immune cells common to most tissues and highly malleable to microenvironmental factors, suggesting that they could function as indicators of distinct pathologic pathways in affected tissues and also serve as targets for tailored treatments in a specific disease. Furthermore, medications can be used to repolarize macrophages into states that actively resolve pathologic responses, as is now being developed for cancer treatment (16, 17). To develop such therapeutics for autoimmune and inflammatory conditions, an in-depth classification of tissue macrophages is needed, along with an understanding of how medications will redirect them as they concurrently react to the tissue environment and pathologic signals.

In the chronically inflamed RA joint tissue, macrophages are a source of TNF, a well-established driver of RA (18–21). However, the precise nature and variety of macrophages within the RA synovium is not yet defined. Furthermore, the cumulative effects of intercellular interactions and medications on macrophage responses in RA tissue remain to be determined.

RESULTS

Single-cell RNA sequencing detects HBEGF$^+$ inflammatory macrophages in RA synovial tissue

To define the spectrum of macrophage phenotypes in a human tissue affected by autoimmunity, we sorted CD14$^+$ cells from the synovial tissue of 10 patients with RA and applied single-cell RNA sequencing (scRNA-seq, CEL-Seq2), as previously reported (22). Two tissue from patients with osteoarthritis (OA) were also included to identify cell subsets that may be found in low frequency in RA tissues, but higher in other disease states. After stringent quality control filtering, 940 CD14$^+$ single cells clustered into four major CD14$^+$ synovial cell subsets based on canonical correlation analysis (CCA) as described (Fig. 1A) (22). Because the cells from all four clusters expressed the myeloid lineage genes *CD68*, *CD163*, *C1QA*, and *CD14* (fig. S1A), we designated these cells macrophages rather than dendritic cells (7, 23). Clusters 1 and 2 contained the majority of the CD14$^+$ cells (45 and 30%, respectively) and the largest number of genes that distinguished them from the other clusters (Fig. 1B and fig. S1B; 125 and 193 genes >2-fold expression difference, respectively). For cluster 1, this included the proinflammatory genes *NR4A3* (nuclear receptor sub-family 4 group A member 3), *PLAUR* (plasminogen activator, urokinase receptor), and *CXCL2* and the growth factors *HBEGF* (heparin binding EGF-like growth factor) and *EREG* (epiregulin) (hereafter referred to as "Cluster 1 HBEGF$^+$") (24, 25).

Author Manuscript Author Manuscript Author Manuscript Author Manuscript

Cluster 2 was marked by a subset of genes involved in phagocytosis, such as *ITGB5*, *ADORA3*, and *MERTK* (Fig. 1B) (26). Cluster 3 appeared less well defined by positive markers, whereas cluster 4 highly expressed a series of IFN-stimulated genes such as *IFI6* and *IFI44L* and herein is referred to as the "IFN/STAT" cluster (Fig. 1B and fig. S1B).

To estimate the abundance of each macrophage cluster in RA tissues, we sorted $CD14^+$ synovial cell populations from 16 patients with RA and 13 patients with OA and analyzed them using bulk RNA-seq (~1000 $CD14^+$ cells from each patient) as previously reported (22). We detected 1726 genes with distinct expression patterns between the two disease states [Fig. 1C, false discovery rate (FDR) adjusted $P < 0.1$], with most of the variation in the samples associated with disease diagnosis (fig. S1C). We detected enrichment of genes and pathways associated with RA disease, such as elevated *TNF STAT1*, and *STAT4* expression and heightened TNF, IFN, and inflammation pathways [gene set enrichment analysis (GSEA)] in RA $CD14^+$ cell populations (Fig. 1C, left and right panel, respectively) (27–30). Overlaying the RA versus OA comparison with markers from each of the single-cell clusters, we found that genes defining the cluster 1 $HBEGF^+$ and cluster 4 IFN/STAT (signal transducer and activator of transcription) macrophages were consistently more abundant in RA $CD14^+$ populations, suggesting an enrichment of these macrophage subsets in RA (Fig. 1D). Furthermore, the cluster 1 $HBEGF^+$ subset was the predominant $CD14^+$ subset found in the majority of RA tissues (fig. S1D; 7 of 12 RA tissues). Cluster 2 genes were found in higher ratios in OA tissues, whereas cluster 3 markers showed no consistent association with either disease (Fig. 1D). RA $CD14^+$ populations were also found to be positively enriched in gene sets generated from cluster 1 $HBEGF^+$ and cluster 4 IFN/STAT while negatively enriched in cluster 2 genes (GSEA, FDR adjusted $P < 0.001$) (Fig. 1E, light gray bars).

To identify factors from the microenvironment that shape synovial macrophage phenotypes, the synovial $CD14^+$ single-cell gene sets were compared to human blood–derived macrophages activated by diverse stimuli (Fig. 1E, colored bars, ranked gene lists). Cluster 1 $HBEGF^+$ and cluster 4 IFN/STAT genes were positively enriched in proinflammatory M1-like macrophage genes induced by TNF and anticorrelated with the IL-4 driven M2 anti-inflammatory phenotype, indicating that these two macrophage subsets are activated by proinflammatory factors (Fig. 1E, red versus yellow bars). Conversely, cluster 2 genes were negatively enriched for TNF-induced inflammatory genes, suggesting that cluster 2 cells are not driven by classic proinflammatory factors. Cluster 2 genes were also not enriched for the IL-4–induced M2 anti-inflammatory polarization program, thereby potentially indicating a distinct macrophage phenotype tailored to factors in the synovial tissue environment. The limited number of cluster 3 positive markers did not significantly associate with any of the stimulated macrophage states. As the most abundant cell type in the RA synovium (31) (fig. S2A), synovial fibroblasts can evoke large shifts in macrophage gene expression profiles (32). The combination of synovial fibroblasts together with TNF (TNF + Fib) generated a macrophage phenotype that aligned closer to cluster 1 $HBEGF^+$ macrophages than the other stimuli (Fig. 1E). This was unlikely due to a simple additive effect that exacerbated the TNF response, as synovial fibroblasts and TNF can induce opposing effects, for example, in cluster 4 genes (Fig. 1E). Thus, we posited that the abundant cluster 1 $HBEGF^+$

Author Manuscript Author Manuscript Author Manuscript Author Manuscript

macrophages from affected human tissue are driven by a combination of tissue-specific factors from resident synovial fibroblasts and inflammatory signals such as TNF.

Consistent with an enrichment in RA, the CD14$^+$ cluster 1 HBEGF$^+$ single cells expressed high amounts of classic inflammatory genes like *IL1B* and low amounts of M2-associating genes such as *MERTK* (Fig. 1, B and F) (13). However, cluster 1 HBEGF$^+$ cells were also distinctively high in the expression of genes such as *HBEGF* and *PLAUR* (Fig. 1F), which have largely been reported as marking anti-inflammatory phenotypes or cells derived from a combination of pro- and anti-inflammatory triggers (33, 34). Considering the unique cluster 1 single-cell phenotype and consistent with elevated *HBEGF* expression across RA CD14$^+$ synovial cell populations (Fig. 1G), we designate cluster 1 macrophages as "HBEGF$^+$ inflammatory macrophages".

In an independent study using a droplet-based scRNA-seq platform (Drop-seq) applied to synovial tissues from five patients with RA (fig. S2A), we detected an abundant macrophage subset with considerable overlap of marker genes with HBEGF$^+$ inflammatory macrophages (fig. S2B, 62%), including *HBEGF*, *PLAUR*, *IL1B*, and *CREM* (fig. S2C) (31). Overlap with the other CD14$^+$ single-cell clusters was less obvious, potentially due to the different technologies and computational and analysis pipelines or to the lower number of samples used in the previous study. Nonetheless, through independent single-cell platforms and patient cohorts, synovial macrophages of the HBEGF$^+$ inflammatory macrophage phenotype can be robustly detected in human tissue affected by RA.

Tissue-resident synovial fibroblasts shape HBEGF$^+$ inflammatory macrophages

To further define the HBEGF$^+$ inflammatory phenotype, we compared the transcriptome of macrophages exposed to TNF and synovial fibroblasts versus TNF alone. In a Transwell coculture system where both cell types were exposed to TNF (24 hours, $n = 4$ donors), synovial fibroblasts altered the expression of 3709 macrophage genes (FDR adjusted $P < 0.1$) (Fig. 2A). The majority of fibroblast-mediated effects opposed the direction of gene expression change induced by TNF alone (Fig. 2A; 69% of fibroblast effects anticorrelated with TNF effects, upper left and lower right). These changes included down-regulation of TNF-inducible proinflammatory mediators such as *CFB*, *CXCL13*, *CCL8*, *MT1H*, *MMP2*, and *SLAMF7* (Fig. 2A, upper left, genes not labeled). Furthermore, fibroblasts up-regulated M2 anti-inflammatory factors that are otherwise suppressed by TNF, including *MRC1*, *MSR1*, and *TREM1* (Fig. 2A, lower right, genes not labeled). Pathway analysis showed that fibroblasts also likely altered the metabolic state of TNF-treated macrophages, indicated by a collective suppression of factors involved in oxidative phosphorylation (fig. S3A).

Despite largely opposing the TNF response, fibroblasts enhanced or permitted TNF induction of a portion of the cluster 1 HBEGF$^+$ genes, including *PLAUR* and *IL8* (Fig. 2A, upper right, red dots). Among HBEGF$^+$ inflammatory genes that TNF alone suppressed, synovial fibroblasts up-regulated *HBEGF*, *RGS2*, and *CREM* [Fig. 2, A (lower right, red dots) and B]. These cluster 1 HBEGF$^+$ markers provide support that, in synovial tissue, fibroblasts reshape the polarization of macrophages by inflammatory factors like TNF. The induction of *HBEGF* by synovial fibroblasts peaked around 12 hours and lasted over the course of days [Fig. 2C; quantitative polymerase chain reaction (qPCR) representative of $n =$

Author Manuscript Author Manuscript Author Manuscript Author Manuscript

4 donors]. The expression of *PLAUR* and the RA-associated transcription factor *STAT4* elevated transiently by TNF alone was hyperinduced by synovial fibroblasts, resulting in a second elongated wave over days (Fig. 2C). Enhanced gene expression correlated with an increase at the protein level for cell surface PLAUR and intracellular STAT4 (Fig. 2, D and E, respectively).

Cross-referencing the fibroblast-induced HBEGF$^+$ macrophage profile with a panel of previously reported macrophage polarization states (12) demonstrated a strong correlation with macrophages treated with TNF and prostaglandin E2 (PGE_2) and/or the Toll-like receptor 2 ligand Pam3-Cys [referred to as "TPP" (12, 35)] (fig. S3B, red text). This strong correlation differed from the weaker or negative correlations with canonical M1 and M2 polarization states (induced by TNF or IFN-γ and IL-4 or IL-13, respectively) (fig. S3B). From these data, we hypothesized that PGE_2 mediated a considerable portion of the synovial fibroblast effect on macrophages. TNF-stimulated synovial fibroblasts (Fig. 2F, F + T) produced large amounts of PGE_2, whereas macrophages produced no detectable PGE_2 irrespective of TNF exposure (Fig. 2F; Mϕ and Mϕ + T). Furthermore, induction of HBEGF$^+$ genes such as *PLAUR* and *HBEGF* in blood-derived macrophages was recapitulated by exogenous PGE_2 and TNF, with the fibroblast-mediated induction blocked by the cyclooxygenase (COX) enzyme inhibitor naproxen (Fig. 2, G and H, respectively). Upon the combination of TNF and PGE_2, the increased transcription of *HBEGF* and *PLAUR* associated with chromatin opening in their promoter regions, as detected by ATAC-seq (assay for transposase-accessible chromatin-seq) and FAIRE-qPCR (formaldehyde-assisted isolation of regulatory elements-qPCR) (Fig. 2, I and J, respectively, and fig. S3C).

These data suggest that in the RA synovium, chronic exposure to the proinflammatory environment results in heightened synovial fibroblast production of prostaglandins that, together with inflammatory factors, drive macrophages toward a state distinct from classical M1 and M2 polarization. Distinct transcriptional regulators, cell surface markers, metabolic pathways, and chromatin modifications mark this HBEGF$^+$ inflammatory state.

HBEGF$^+$ inflammatory macrophages promote fibroblast invasiveness

To examine how HBEGF$^+$ inflammatory macrophages may affect RA pathology, we focused on their intercellular relationship with synovial fibroblasts. In an RNA-seq analysis, exposure to HBEGF$^+$ inflammatory macrophages altered 855 synovial fibroblast genes (FDR adjusted $P < 0.1$), including induction of *IL11*, *LIF*, *CSF3* [granulocyte colony-stimulating factor (GCSF)], *IL33*, *IL6*, and *PLAU* (Fig. 3A). Pathway analyses revealed an up-regulated epidermal growth factor receptor (EGFR) response in the fibroblasts, observed with two gene sets (one induced by EGFR ligands and a second blocked by an EGFR inhibitor) (Fig. 3B). Similar to the gene expression changes, we also detected increased GCSF and IL-33 protein in culture supernatants in the presence of HBEGF$^+$ macrophages (Fig. 3C). The increased production of neutrophil chemoattractants and growth factors, such as GCSF, led us to investigate how HBEGF$^+$ inflammatory macrophages may affect neutrophils. Supernatants from cocultures of HBEGF$^+$ macrophages and synovial fibroblasts resulted in elevated neutrophil counts in a culture-based viability assay (fig. S4A). As synovial fluid from inflamed RA joints is characterized by elevated neutrophils (36, 37),

Author Manuscript Author Manuscript Author Manuscript Author Manuscript

increased production of neutrophil chemoattractant and survival factors in the tissue may support neutrophil recruitment and viability as they transit into the synovial fluid. Last, we found that the expression of *GCSF* and *IL33* was sensitive to EGFR inhibition (AG-1478, AG) (Fig. 3D), further implicating EGFR involvement in this inflammatory macrophage-fibroblast cross-talk system and identifying an additional therapeutic avenue to target HBEGF$^+$ macrophage-driven inflammation.

To further understand the EGFR responses in the synovial fibro-blasts, we investigated the expression of EGF ligands and EGFR subunits in both the macrophages and fibroblasts in the coculture system and in primary synovial macrophages and fibroblasts. Synovial fibroblasts expressed only trace amounts of seven EGF ligands with no change in response to TNF and HBEGF$^+$ macrophages (fig. S4B). In contrast, macrophages induced *HBEGF* and a second EGF ligand *EREG* upon combined exposure to TNF and synovial fibroblasts (fig. S4B). Although *EREG* expression in the blood-derived macrophage system was higher than that of *HBEGF* (fig. S4B), the RA patient synovial macrophages exhibited considerably higher expression of *HBEGF* (Fig. 1B). For EGFR expression, synovial fibroblasts expressed two subunits (EGFR and ERBB2), whereas neither blood-derived macrophages nor RA synovial macrophages expressed EGFR subunits (fig. S4, C and D). Considering these data, we posit that synovial fibroblast EGFR responses arise in response to EGF ligand expressed by fibroblast-entrained inflammatory HBEGF$^+$ macrophages.

EGFR signaling is a robust regulator of fibroblast motility (38). In RA, synovial fibroblasts contribute to the invasion and destruction of cartilage and bone by synovium (39–42). Thus, we next tested whether a heightened EGF response influenced the migration of synovial fibroblasts through extracellular matrix. Preincubation of fibroblasts with TNF and macrophages induced a pronounced increase in fibroblast invasiveness that was mitigated by EGF receptor inhibition (Fig. 3E and fig. S4E). These data demonstrate that the HBEGF$^+$ macrophage-dependent EGFR response may promote pathologic fibroblast-mediated and pannus-associated tissue destructive behaviors in RA joints.

RA medications target HBEGF$^+$ inflammatory macrophage polarization

We next examined how clinically effective RA medications affect the polarization of HBEGF$^+$ inflammatory macrophages, using human blood–derived macrophages exposed to TNF and synovial fibro-blasts. In comparison to macrophages exposed only to TNF, the presence of synovial fibroblasts substantially altered the effects of most medications (fig. S5A). For example, the majority of auranofin targets were lost when macrophages were polarized toward the HBEGF$^+$ phenotype (1300 genes, 67%) (fig. S5A, blue versus yellow). In contrast, several of the medications gained more than 1000 gene targets in HBEGF$^+$ inflammatory macrophages, including naproxen and leflunomide (A77, an active leflunomide metabolite) (fig. S5A). In macrophages exposed only to TNF, induction of nuclear factor κB (NF-κB) target genes was reversed by auranofin and several other medications, but not by naproxen and leflunomide (fig. S5B). However, synovial fibroblast-mediated suppression of Myc target genes in TNF-induced macrophages was reversed by naproxen and leflunomide (fig. S5C). Thus, synovial fibroblasts alter the response of macrophages to medications used to treat patients with RA.

Author Manuscript Author Manuscript Author Manuscript Author Manuscript

Several medications reversed a large portion of fibroblast-induced effects (~1000 genes), suggesting that the efficacy of these treatments in the clinic could involve a suppression of HBEGF$^+$ inflammatory macrophages in the RA synovium (Fig. 4A, black bars). This included leflunomide (A77), dexamethasone (steroid), naproxen, and triple therapy (Tri, hydroxychloroquine + sulfasalazine + methotrexate) (Fig. 4A, black bars). Naproxen inhibits COX enzyme-mediated prostaglandin production and, in our assay, affected the majority of genome-wide fibroblast-mediated effects (~80%) (Fig. 4A and fig. S5, A to D), further supporting the idea that prostaglandins are a dominant fibroblast product driving HBEGF$^+$ inflammatory macrophages. The inhibition of HBEGF$^+$ inflammatory macrophages by various medications resulted in at least two functionally distinct states. Naproxen, for example, blocked the prostaglandin arm driving HBEGF$^+$ inflammatory macrophages, but still permitted TNF polarization of the macrophages toward an M1-like proinflammatory phenotype, which presumably also functions pathologically in RA synovium (fig. S5, A and D). In contrast, medications like dexamethasone were capable of largely blocking both the TNF and PGE_2 responses (fig. S5A), driving macrophages closer to an untreated/naïve-like phenotype. These results highlight the importance of understanding variations in macrophage phenotypes after treatment, particularly in complex tissue settings where multiple factors could redirect macrophages toward a differing yet pathologic state.

RA medications target the HBEGF$^+$ macrophage-synovial fibroblast axis in patient samples

To study the therapeutic targeting of HBEGF$^+$ macrophages in RA joints, we directly assayed synovial tissue from patients with RA (43, 44) that contained extensive lymphocyte infiltration (45, 46) (table S1; $n = 8$). Specifically, in an ex vivo tissue assay, synovium was dissociated into cell suspensions (47) and cultured with U.S. Food and Drug Administration (FDA)–approved RA medications (Fig. 4B). Similar to the seminal assays that laid the precedent for effective anti-TNF therapies in RA (48–50), exposure to anti-TNF antibodies (adalimumab) suppressed production of the inflammatory mediator IL-1β (Fig. 4C). Furthermore, in this assay, the Janus kinase (JAK) inhibitor tofacitinib imparted notable reductions in genome-wide IFN-α responses and secreted protein for the JAK/STAT target *CXCL10* (IP10) (Fig. 4C). Anti-inflammatory therapies such as anti-TNF, tofacitinib, and dexamethasone inhibited the HBEGF$^+$ inflammatory synovial macrophage cluster 1 gene set (Fig. 4D). Conversely, the panel of anti-inflammatory medications up-regulated the cluster 2 gene set (with one exception, A77/leflunomide) (Fig. 4D), including anti-inflammatory genes *MERTK*, *TGFBI*, and *MARCO* (Fig. 1F and fig. S5E) (51–53). Tofacitinib was the most potent inhibitor of the cluster 4 IFN/STAT gene set (Fig. 4D), further implicating a robust JAK/STAT response in this RA-associated macrophage subset. The JAK/STAT response in cluster 4 was induced by naproxen, as indicated by an enrichment of cluster 4 genes and elevated *CXCL10*/IP10 protein production in naproxen-treated RA synovial cells (Fig. 4, D and E). This was associated with a reduction in prostaglandin production upon treatment with naproxen (Fig. 4F) and is in accord with the established inhibitory effects of prostaglandins on IFN responses (54–56).

To test for evidence of the cross-talk module we identified between HBEGF$^+$ inflammatory macrophages and synovial fibroblast EGFR responses, we further examined the effects of naproxen in our tissue explant system. Here, we found that naproxen blocked prostaglandin

Author Manuscript Author Manuscript Author Manuscript Author Manuscript

production and reduced *HBEGF* expression and GCSF (*CSF3*) protein secretion by the RA synovial explants (Fig. 4, F to H), indicating a decoupling of the macrophage-fibroblast circuit. Naproxen did not interfere with TNF-mediated effects in the ex vivo tissue assay, as indicated by the lack of change in IL-1β protein production (Fig. 4I). TNF blockade with adalimumab in the ex vivo tissue assay, however, was effective in blocking both *HBEGF* expression and IL-1β protein production (Fig. 4, C and D), thereby derailing generation of both the HBEGF$^+$ inflammatory macrophages and proinflammatory M1-like macrophages (fig. S5F).

To directly assay EGFR-dependent fibroblast gene expression changes consistent with HBEGF$^+$ inflammatory macrophage influence, we introduced a therapeutic EGFR inhibitor not currently used to treat RA into the ex vivo assay. The EGFR inhibitor reversed the majority of the synovial fibroblast gene expression effects elicited by HBEGF$^+$ inflammatory macrophages (77%), including a suppression of *CCL20*, *CSF3*, *LIF*, *IL33*, *IL11*, and *PLAU* (Figs. 3A and 4J). Together, these data provide evidence within patient tissues for the cross-talk module we identified between HBEGF$^+$ inflammatory macrophages and tissue-resident fibroblasts and furthermore indicate that blockade of EGFR responses may provide a nonimmuno-suppressive therapeutic approach for RA.

DISCUSSION

Challenges in treating autoimmune and inflammatory disorders have led to strategies including administering medications sequentially until one is found to improve clinical symptoms. In an effort to improve a priori knowledge of which medication will be most effective, we have taken into consideration the cellular interactions in affected tissues, identifying a population of HBEGF$^+$ inflammatory macrophages in inflamed RA joints and delineating their deterministic tissue-resident and disease-specific factors. Furthermore, we have identified medications that successfully interfere with the generation of these macrophages and the support they provide toward fibroblast invasiveness, which contributes to irreversible joint destruction in RA.

The cross-talk mechanisms and functional output between macrophages and fibroblasts in the RA tissue environment differ from other pathologic states driven by these two cell types. In fibrosis, macrophages and fibroblasts drive excessive collagen deposition, blocking tissue function in part by static physical barriers rather than invasive and erosive behaviors (2, 57, 58). In RA, fibroblast products such as prostaglandins combine with chronic inflammatory signals such as TNF to polarize macrophages into a state that is distinct from inflammatory M1, anti-inflammatory wound healing M2, and profibrotic transforming growth factor-β–expressing macrophages. The RA-enriched HBEGF$^+$ inflammatory macrophages produce a defined subset of inflammatory products such as IL-1 and the EGF growth factors HB-EGF and epiregulin. Because HBEGF$^+$ inflammatory macrophages subsequently induce invasiveness in synovial fibro-blasts, we classify them as “proinvasive macrophages.”

Although leukocyte-derived growth factors have emerged as critical components in tissue homeostasis and repair (1, 59), our data uncovered a pathologic correlate. In the RA tissue environment, macrophage-produced EGF ligands lead to EGFR-dependent synovial

Author Manuscript Author Manuscript Author Manuscript Author Manuscript

fibroblast invasiveness and GCSF production concomitant with enhanced neutrophil accumulation—dominant features of RA joint pathology (36, 37, 40). In inflammatory arthritis in vivo models, disease progression is driven by EGF ligands, EGF receptor activity, and the enzyme iRhom2, which mediates release of both TNF and HB-EGF from immune cells (60–63). Our data provide relevance to these findings in human disease and a mechanistic understanding of the cellular cross-talk involving growth factors in RA joints. TNF and HB-EGF have been implicated as pathologic drivers of kidney disease in the autoimmune condition lupus (64, 65). Thus, linked TNF and EGFR responses may be a unifying and targetable feature in tissues affected by disparate autoimmune conditions.

Using perturbations relevant to human disease, namely, FDA-approved medications, we have detailed the disruption of intercellular interactions in patient samples and the resulting cellular phenotypes, thereby gaining insights into the complex consequences of medications on RA joint tissue. Our data yielded insights into a long-standing question of why anti-inflammatory COX inhibitors known as NSAIDs are not “disease modifying” in RA (15). Our data suggest that NSAIDs, like naproxen, block the prostaglandin-mediated arm in $HBEGF^+$ inflammatory macrophage polarization, but still permit macrophage TNF responses. Thus, NSAID therapy in RA likely redirects $HBEGF^+$ inflammatory macrophages toward a classic proinflammatory M1-like phenotype, which would presumably perpetuate inflammation, albeit through a different pathway. In that regard, NSAIDs may best be used in combination with medications like anti-TNFs to most effectively target $HBEGF^+$ inflammatory macrophage polarization. However, COX inhibition by naproxen may also prove problematic in the other RA-enriched macrophage phenotype, by inducing the cluster 4 IFN/STAT response, consistent with the previously documented and robust suppression of IFN responses by prostaglandins (54, 56). Thus, NSAIDs are permissive of pathologic responses for two RA-enriched macrophage phenotypes. These data speak to the greater need to understand tissue microenvironment factors that polarize macrophages and how, in the presence of therapeutics, the intercellular communication networks are rewired and subsequently repolarize macrophages into states that either resolve or perpetuate pathology.

Limitations of this study include the inability of an in vitro coculture system to fully recapitulate all aspects of a macrophage phenotype found within human synovial tissue. Furthermore, although an in vitro assay can measure fibroblast invasiveness, a precise understanding of how this translates into fibroblast activity within patient synovial tissue is limited. The in vitro and ex vivo drug assays have limitations related to differences in how medications are processed in cultured cells versus the human body, including how drugs are metabolized in the intestinal tract and their stabilization upon binding to carrier proteins in the blood, among others. Last, the analysis of macrophage responses in the ex vivo tissue assay is derived from mixed synovial cell RNA-seq data and thereby may be incorporating expression changes from other synovial cell types.

Along with the seminal synovial explant assay that provided the rationale for use of TNF therapies in RA (48), our work supports the implementation of ex vivo assays to better understand and treat patients with autoimmune and inflammatory disorders. Specifically, in addition to detecting genome-wide established targets of anti-TNF and tofacitinib therapies,

Author Manuscript Author Manuscript Author Manuscript Author Manuscript

our RA patient ex vivo synovial tissue bioassay provides a human- and disease-relevant system that unmasked the interconnectivity and drug responsiveness of the synovial macrophage-fibroblast interaction we identified. Human tissue–based therapeutic testing for autoimmune conditions may offer guidance in defining personalized therapies, as the intercellular networks driven by the unique cellular composition in a patient's tissue may be exploited in ex vivo assay to indicate how these cells cross-regulate after treatment with a medication and collectively shape new tissue responses. For RA, this could be accomplished with the expanding use of synovial biopsies (21, 22, 66) and ultimately with the identification of circulating biomarkers that correlate with tissue-based assays. Last, effective blockade of the macrophage-induced fibroblast response in the RA tissue ex vivo assay with an EGFR inhibitor developed for cancer warrants testing of this as a new treatment direction, particularly because it may not broadly suppress the immune system, unlike many of the current RA medications.

MATERIALS AND METHODS

Study design

The objectives of this project were to study macrophage phenotypes that are enriched in the joints of patients with the autoimmune disease RA using scRNA-seq and to understand how medications affect these phenotypes using ex vivo tissue assays. An in vitro coculture model system was used to understand how resident synovial cell types and pathologic cytokines drive macrophage phenotypes and drug responses. Synovial tissue from patients treated for RA and OA was used, in addition to blood from healthy human donors. All patients were consented under institutional review board (IRB) – approved studies at Hospital for Special Surgery or clinical sites in the Accelerating Medicines Partnership (AMP) consortium. Inclusion and exclusion criteria for patients with arthritis were based on standard clinical diagnostic criteria, such as the ACR 2010 RA criteria. Perceived outliers in sequencing datasets from the coculture system remained in the analyses upon application of surrogate variable analysis by svaseq version 3.26.0. The number of human donor blood-derived macrophage biologic replicates depended on the robustness of the response for each type of assay and therein the variability across donors: For robust assay responses, typically about $n = 4$ donors were used, whereas for assays with higher variability, $n = 8$ donors were used. Individual subject-level data are provided in data file S1.

Patient recruitment and CD14$^+$ synovial cell sorting for RNA-seq

The multicenter RA/SLE (systemic lupus erythematosus) Network of the AMP consortium enrolled individuals meeting the ACR 2010 RA classification according to protocols approved by the IRB at each site (22, 47). Synovial tissues were collected from ultrasound-guided biopsies or joint replacement surgery and viably frozen in CryoStor CS10 cryopreservation media (Sigma-Aldrich). At a central processing site, tissues were dissociated and cells were FACS (fluorescence-activated cell sorting)–sorted (BD FACSAria Fusion) into fibroblast, macrophage, B cell, and T cell populations. Macrophages were sorted on the basis of CD14$^+$CD45$^+$ cell surface expression. For bulk RNA-seq on CD14$^+$ synovial cell populations, ~1000 cells were sorted directly into RNeasy RLT lysis buffer

Author Manuscript Author Manuscript Author Manuscript Author Manuscript

(Qiagen). For $CD14^+$ synovial scRNA-seq, ~100 live cells per patient were individually plated and lysed in 384-well plates.

Bulk RNA-seq and scRNA-seq of sorted $CD14^+$ synovial cells

For bulk populations of cells, full-length complementary DNA and sequencing libraries were generated using Illumina Smart-Seq2 protocol (67). Libraries were sequenced on a MiSeq System (Illumina) to generate 35–base pair, paired-end reads. scRNA-seq was performed on sorted macrophage and synovial fibroblast using the CEL-Seq2 protocol (68) in 384-well plates. Libraries were sequenced on a HiSeq 2500 (Illumina) in rapid run mode to generate 76–base pair, paired-end reads.

$CD14^+$ bulk RNA-seq read alignment and differential gene expression analysis

Reads were aligned and quantified with STAR version 2.4.2a (69) against the GRCh38 genome and GENCODE Release 27 annotation, respectively. Differential expression analyses and batch correction were performed using DESeq2 (70) version 1.18.1 and svaseq (71) version 3.26.0, respectively.

$CD14^+$ scRNA-seq read alignment and differential gene expression analysis

RNA-seq reads were aligned with STAR version 2.5.2b (69) to the hg19 reference genome. Transcript levels were quantified as CPM using the GENCODE Release 24 annotation. The single-cell gene expression matrix was clustered based on a CCA methodology (22). Briefly, scRNA-seq and bulk RNA-seq datasets were integrated based on the highly variable genes that maximized the correlation between the two datasets. The correlated canonical variates were then used to construct a nearest-neighbor network, thereby generating clusters that are verified to be present in the bulk data. Using the four clusters identified from the CCA method, the top 10 canonical coordinates were used to generate a Euclidean distance matrix for t-distributed stochastic neighbor embedding (t-SNE) visualization using a perplexity parameter of 40. Positive and negative cluster markers were identified using the Wilcoxon rank sum test with a Bonferroni correction for multiple testing.

Pathway analysis

Gene lists were processed for GSEA (72) version 3.0 by taking the inverse of the FDR adjusted *P* value for each gene and multiplying it by the sign of the $\log_2$ fold change relative to the baseline conditions. GSEA was run under the "pre-rank" mode with 1000 permutations for each of the gene sets available in MSigDB and ImmunSigDB version 5.2. Additional pathway analysis was performed using QIAGEN's Ingenuity Pathway Analysis (IPA, QIAGEN Redwood City, www.qiagen.com/ingenuity). Reported pathways were referenced as follows with the MSigDB systematic name in parentheses: TNF-α signaling via NF-κB (M5890), IFN-γ response (M5913), IFN-α response (M5911), inflammation (M5932), Myc targets (M5926 and M5928), oxidative phosphorylation (M5936), translation (M11989), cell cycle (M543), induced by EGF (M2613), hypoxia-induced (M5891), IFN-responsive genes (M9221), EGFR inhibitor (M16010), and KEGG (Kyoto Encyclopedia of Genes and Genomes) ribosome pathway (M189). Gene sets derived from the $CD14^+$ synovial scRNA-seq markers were composed of up to 500 genes that exhibited >0.5 $\log_2$

Author Manuscript Author Manuscript Author Manuscript Author Manuscript

fold change (positive marker) or <−0.5 $\log_2$ fold change (negative marker genes) relative to all other clusters, sorted by their fold change.

Independent RA arthroplasty cohort analyzed by Drop-seq

In an independent analysis, we collected synovial tissue from five RA patients consented under Hospital for Special Surgery (HSS) RA Studies (IRB nos. 2014–317 and 2014–233) during arthroplasty and synovectomy procedures. Tissues were dissociated into single-cell preparations, and all cells were run through a Drop-seq protocol and sequenced on a HiS-eq 2500 (Illumina) (31). After cell and gene filtering (31), we applied Seurat version 2.3.0 to generate principal components analysis–based single-cell clusters, which were labeled on the basis of cell-type markers. A total of 20,031 single cells were visualized using the t-SNE implementation in Seurat using a perplexity parameter of 20 and 13 principal components. After identifying a macrophage cluster consistent with our previous results (4212 single cells), we reapplied Seurat and identified distinct subpopulations and visualized in t-SNE space.

Cell culture for human blood–derived macrophages and synovial fibroblasts

Human $CD14^+$ monocytes were purified from leukocyte preparations purchased from the New York Blood Center and differentiated into blood-derived macrophages for 1 to 2 days in macrophage CSF (M-CSF; 10 ng/ml) (PeproTech) and RPMI 1640 medium (Life Technologies)/10% defined fetal bovine serum (FBS) (HyClone). Cells were stimulated with recombinant human TNF (20 ng/ml) (PeproTech). Drug treatments were administered 15 min after TNF exposure to both the top and bottom wells of the Transwell system to achieve the stated final concentrations. After suspending in dimethyl sulfoxide according to the company's instructions, auranofin (Sigma-Aldrich) was added to cells at 500 nM, A77 1726 (Santa Cruz Biotechnology) was added at 50 mM, Tyrphostin AG 1478 (Sigma-Aldrich) was added at 4 μM, GW 627368X (Cayman Chemical) was added at 10 μM, sulfasalazine (Sigma-Aldrich) was added at 3 μM, hydroxychloroquine sulfate (Sigma-Aldrich) was added at 50 μM, methotrexate (Cayman Chemical) was added at 110 μM, tofacitinib citrate (Cayman Chemical) was added at 1 μM (73), and Pam3CSK4 (InvivoGen) was added at 1000 μg/ml. Dexamethasone (Sigma-Aldrich) and PGE_2 (Sigma-Aldrich) were first suspended in absolute ethanol and then added to cells (100 and 280 nM, respectively). Naproxen was suspended in RPMI 1640 supplemented with 10% FBS and then added to cells at a final concentration of 100 μM. Anti-TNF was provided as adalimumab and was added to cells at a final concentration of 50 μg/ml.

Human synovial fibroblasts derived from deidentified synovial tissues of RA patients undergoing arthroplasty (HSS IRB no. 14–033). Dissociated cells were plated in α-minimum essential medium (α-MEM)–based media up to 10 days, washing with media numerous times to remove dying blood cell components. Synovial fibroblasts at passages 4 to 6 were used for experiments. The diagnoses of RA were based on the ACR 2010 criteria. For Transwell culture experiments, synovial fibroblasts adhered to polyester chambers with 0.4-μm pores (Corning) and were suspended above the wells containing macrophages, with a fibroblast-to-macrophage ratio of 1:16 on the basis of the size of the cells and their coverage of the culture well surface. The number of donors used for each experiment is listed in the

Author Manuscript Author Manuscript Author Manuscript Author Manuscript

figure legend and refers to unique donors for both the blood-derived macrophages and the synovial fibroblast lines.

RNA-seq for human blood–derived macrophages and synovial fibroblasts

Total RNA was extracted using the RNeasy mini kit (Qiagen). TruSeq (nonstranded) sample preparation kits (Illumina) were used to purify poly(A) transcripts and generate libraries with multiplexed barcode adaptors. Single-end libraries were multiplexed, pooled, and sequenced using the Single Read Clustering with 50 or 100 cycles on an Illumina HiSeq 4000. Sequencing was performed by the Weill Cornell Medical College Genomics Resources Core Facility. RNA-seq read alignment, quantification, differential testing, and pathway analysis were performed as described in previous sections.

Fibroblast invasion assay

Human synovial fibroblasts were plated in Transwell inserts with macrophages below as described above for the Transwell experiments. AG 1478 (Sigma-Aldrich) was added at 4 μM for the 32-hour coculture incubation. Fibroblasts were trypsinized and replated in 500 μl of plain α-MEM with M-CSF (10 ng/ml) at 0.1×10^6 cells per well into 24-well Corning BioCoat Matrigel Invasion Chambers. Macrophages were resuspended in 750 μl of plain α-MEM and seeded underneath invasion Transwells in the appropriate conditions. AG 1478 was added at a concentration of 4 μM; after 18 hours, the fibroblasts were fixed for 10 min in ice-cold methanol and stained using crystal violet. Invasive fibroblast numbers were quantified via light microscopy.

Human RA ex vivo synovial cell assays

For synovial cell cultures, RA patient synovial tissue was obtained from patients consented into the HSS FLARE study (IRB no. 2014–233). Tissues were digested with Liberase TL (100 mg/ml, Roche) and deoxyribonuclease I (100 μg/ml, Roche) for 15 min and passed through three 70 μM cell strainers. Cells were then suspended in 1 ml of red blood cell lysis buffer (gift of J. Lederer, BWH) for 3 min followed by addition of RPMI 1640/10% FBS/1% glutamine to quench the reaction. Disaggregated synovial cells were plated in RPMI 1640/10% FBS/1% glutamine at 0.2×10^6 in 96-well plates. Cells were treated with drugs at aforementioned concentrations for 24 hours. Supernatants and RNA were collected for Luminex experiments and qPCR, respectively. For RNA-seq, the samples were multiplexed in eight samples per lane, 50 cycles, single-end reads, with TruSeq (Illumina) for library prep and a HiSeq 4000 (Illumina) in the Weill Cornell Medical College Genomics Resources Core Facility. RNA-seq read alignment, quantification, differential testing, and pathway analysis were performed as described in previous sections.

Statistical analysis

scRNA-seq clusters were identified using a graph-based clustering method based on CCA (22). Markers for different clusters were determined by Bonferroni-corrected Wilcoxon rank sum tests implemented in Seurat version 2.3.0. Visualization of intersecting sets was performed using UpSetR version 1.3.3 (74). Testing for differentially expressed genes from bulk RNA-seq count data was performed using DESeq2 version 1.18.1 and surrogate

Author Manuscript Author Manuscript Author Manuscript Author Manuscript

variable analysis was performed using svaseq version 3.26.0, both run on the R version 3.3.2. All RNA-seq significance levels are reported as FDR adjusted *P* values. Spearman and Pearson correlation analysis was performed using the seaborn statistical data visualization package version 0.8.1 run on Python version 3.6.4. Statistical significance of pathway analysis was reported as the normalized enrichment score and FDR adjusted *P* values determined from testing of 1000 permutations from GSEA version 3.0. Pathway *z* scores for upstream regulatory analyses were performed using IPA (QIAGEN). Data from in vitro and ex vivo assays are shown as mean ± SE unless stated otherwise. Two-tailed paired *t* tests were performed for human sample–derived qPCR and ELISA data using GraphPad Prism version 5.04 for Windows. Luminex multiplex ELISA experimental data were tested for normality by the Shapiro-Wilk test with a significance threshold of $P < 0.05$ and were found to not follow a Gaussian distribution. Subsequent statistical analysis was thus performed by Wilcoxon signed rank tests, a nonparametric method, using GraphPad Prism.

Supplementary Material

Refer to Web version on PubMed Central for supplementary material.

Acknowledgments:

We thank HSS orthopedic surgeons (particularly M. Figgie), rheumatologists, clinical research coordinators (particularly R. Cummings, M. McNamara, and S. Mirza), and the HSS patients; P. Gulko and T. Laragione (Mt. Sinai) for technical guidance on synovial fibroblast invasion assays; R. Yuan and E. Giannopoulou for assistance with sequencing data; and C. Blobel and H. Hang for critically reading the manuscript. We also acknowledge R. Satija, W. Stephenson, and A. Butler of the New York Genome Center for their previous collaboration and the data used here from a synovial tissue single-cell analysis using Drop-seq technology (31). We acknowledge the AMP RA/SLE Network for the large-scale collection of arthritis patient synovial tissues, cell sorting, and RNA-seq. AMP is a public-private partnership (AbbVie, Arthritis Foundation, Bristol-Myers Squibb, Lupus Foundation of America, Lupus Research Alliance, Merck Sharp & Dohme, NIH, Pfizer, Rheumatology Research Foundation, Sanofi, and Takeda Pharmaceuticals International) created to develop new ways of identifying and validating promising biologic targets for diagnostics and drug development. Individuals from academic medical centers include the following: J. Albrecht, J. H. Anolik, W. Apruzzese, M. B. Brenner, S. L. Bridges Jr., B. F. Boyce, D. L. Boyle, C. D. Buckley, J. H. Buckner, V. P. Bykerk, E. DiCarlo, J. Dolan, L.T. Donlin, T. M. Eisenhaure, A. Filer, G. S. Firestein, C. Y. Fonseka, E. M. Gravallese, P. K. Gregersen, S. M. Goodman, J. M. Guthridge, M. Gutierrez-Arcelus, N. Hacohen, V. M. Holers, L. B. Hughes, L. B. Ivashkiv, E. A. James, J. A. James, A. H. Jonsson, J. Keegan, S. Kelly, Y. C. Lee, J. A. Lederer, D. J. Lieb, A. M. Mandelin II, M. J. McGeachy, M. A. McNamara, J. R. Mears, F. Mizoguchi, L. Moreland, J. P. Nguyen, A. Noma, C. Nusbaum, D. E. Orange, N. M. Pellett, H. Perlman, C. Pitzalis, J. Rangel-Moreno, D. A. Rao, M. Rohani-Pichavant, S. Raychaudhuri, C. Ritchlin, W. H. Robinson, C. Rozo, K. Salomon-Escoto, J. Seifert, A. Seshadri, K. Slowikowski, D. Sutherby, P. J. Utz, D. Tabechian, J. D. Turner, G. F. M. Watts, K. Wei, and F. Zhang.

Funding:

Funding was provided by the NIH grants UH2-AR-067676, UH2-AR-067677, UH2-AR-067679, UH2-AR-067681, UH2-AR-067685, UH2-AR-067688, UH2-AR-067689, UH2-AR-067690, UH2-AR-067691, UH2-AR-067694, and UM2-AR-067678 (AMP RA/SLE Network); MSKCC core funding (G.R.) and ETH Zurich core funding (G.R.); RO1AR046713, AR050401, and AI046712 (L.B.I.); and the Ambrose Monell Foundation (L.T.D.) and K01AR066063 (L.T.D.).

REFERENCES AND NOTES

1. Rankin LC, Artis D, Beyond host defense: Emerging functions of the immune system in regulating complex tissue physiology. Cell 173, 554–567 (2018). [PubMed: 29677509]
2. Wynn TA, Chawla A, Pollard JW, Macrophage biology in development, homeostasis and disease. Nature 496, 445–455 (2013). [PubMed: 23619691]

Author Manuscript Author Manuscript Author Manuscript Author Manuscript

3. Lavin Y, Winter D, Blecher-Gonen R, David E, Keren-Shaul H, Merad M, Jung S, Amit I, Tissue-resident macrophage enhancer landscapes are shaped by the local microenvironment. Cell 159, 1312–1326 (2014). [PubMed: 25480296]
4. Okabe Y, Medzhitov R, Tissue biology perspective on macrophages. Nat. Immunol 17, 9–17 (2016). [PubMed: 26681457]
5. Gosselin D, Link VM, Romanoski CE, Fonseca GJ, Eichenfield DZ, Spann NJ, Stender JD, Chun HB, Garner H, Geissmann F, Glass CK, Environment drives selection and function of enhancers controlling tissue-specific macrophage identities. Cell 159, 1327–1340 (2014). [PubMed: 25480297]
6. Ginhoux F, Guilliams M, Tissue-resident macrophage ontogeny and homeostasis. Immunity 44, 439–449 (2016). [PubMed: 26982352]
7. Gautier EL, Shay T, Miller J, Greter M, Jakubzick C, Ivanov S, Helft J, Chow A, Elpek KG, Gordonov S, Mazloom AR, Ma'ayan A, Chua WJ, Hansen TH, Turley SJ, Merad M, Randolph GJ, Immunological Genome Consortium, Gene-expression profiles and transcriptional regulatory pathways that underlie the identity and diversity of mouse tissue macrophages. Nat. Immunol 13, 1118–1128 (2012). [PubMed: 23023392]
8. Hulsmans M, Clauss S, Xiao L, Aguirre AD, King KR, Hanley A, Hucker WJ, Wülfers EM, Seemann G, Courties G, Iwamoto Y, Sun Y, Savol AJ, Sager HB, Lavine KJ, Fishbein GA, Capen DE, Da Silva N, Miquerol L, Wakimoto H, Seidman CE, Seidman JG, Sadreyev RI, Naxerova K, Mitchell RN, Brown D, Libby P, Weissleder R, Swirski FK, Kohl P, Vinegoni C, Milan DJ, Ellinor PT, Nahrendorf M, Macrophages facilitate electrical conduction in the heart. Cell 169, 510–522.e20 (2017). [PubMed: 28431249]
9. Keren-Shaul H, Spinrad A, Weiner A, Matcovitch-Natan O, Dvir-Szternfeld R, Ulland TK, David E, Baruch K, Lara-Astaiso D, Toth B, Itzkovitz S, Colonna M, Schwartz M, Amit I, A unique microglia type associated with restricting development of Alzheimer's disease. Cell 169, 1276–1290 (2017). [PubMed: 28602351]
10. Witztum JL, Lichtman AH, The influence of innate and adaptive immune responses on atherosclerosis. Annu. Rev. Pathol 9, 73–102 (2014). [PubMed: 23937439]
11. Pagán AJ, Ramakrishnan L, Immunity and immunopathology in the tuberculous granuloma. Cold Spring Harb. Perspect. Med 5, a018499 (2014). [PubMed: 25377142]
12. Xue J, Schmidt SV, Sander J, Draffehn A, Krebs W, Quester I, De Nardo D, Gohel TD, Emde M, Schmidleithner L, Ganesan H, Nino-Castro A, Mallmann MR, Labzin L, Theis H, Kraut M, Beyer M, Latz E, Freeman TC, Ulas T, Schultze JL, Transcriptome-based network analysis reveals a spectrum model of human macrophage activation. Immunity 40, 274–288 (2014). [PubMed: 24530056]
13. Locati M, Mantovani A, Sica A, Macrophage activation and polarization as an adaptive component of innate immunity. Adv. Immunol 120, 163–184 (2013). [PubMed: 24070384]
14. Neurath MF, Cytokines in inflammatory bowel disease. Nat. Rev. Immunol 14, 329–342 (2014). [PubMed: 24751956]
15. Crofford LJ, Use of NSAIDs in treating patients with arthritis. Arthritis Res. Ther 15 (suppl. 3), S2 (2013).
16. Pyonteck SM, Akkari L, Schuhmacher AJ, Bowman RL, Sevenich L, Quail DF, Olson OC, Quick ML, Huse JT, Teijeiro V, Setty M, Leslie CS, Oei Y, Pedraza A, Zhang J, Brennan CW, Sutton JC, Holland EC, Daniel D, Joyce JA, CSF-1R inhibition alters macrophage polarization and blocks glioma progression. Nat. Med 19, 1264–1272 (2013). [PubMed: 24056773]
17. Cassetta L, Kitamura T, Targeting tumor-associated macrophages as a potential strategy to enhance the response to immune checkpoint inhibitors. Front. Cell Dev. Biol 6, 38 (2018). [PubMed: 29670880]
18. Udalova IA, Mantovani A, Feldmann M, Macrophage heterogeneity in the context of rheumatoid arthritis. Nat. Rev. Rheumatol 12, 472–485 (2016). [PubMed: 27383913]
19. Kalliolias GD, Ivashkiv LB, TNF biology, pathogenic mechanisms and emerging therapeutic strategies. Nat. Rev. Rheumatol 12, 49–62 (2016). [PubMed: 26656660]
20. McInnes IB, Schett G, The pathogenesis of rheumatoid arthritis. N. Engl. J. Med 365, 2205–2219 (2012).

Author Manuscript Author Manuscript Author Manuscript Author Manuscript

21. Mandelin II AM, Homan PJ, Shaffer AM, Cuda CM, Dominguez ST, Bacalao E, Carns M, Hinchcliff M, Lee J, Aren K, Thakrar A, Montgomery AB, Louis Bridges S Jr., Bathon JM, Atkinson JP, Fox DA, Matteson EL, Buckley CD, Pitzalis C, Parks D, Hughes LB, Geraldino-Pardilla L, Ike R, Phillips K, Wright K, Filer A, Kelly S, Ruderman EM, Morgan V, Abdala-Valencia H, Misharin AV, Budinger GS, Bartom ET, Pope RM, Perlman H, Winter DR, Transcriptional profiling of synovial macrophages using minimally invasive ultrasound-guided synovial biopsies in rheumatoid arthritis. Arthritis Rheumatol 70, 841–854 (2018). [PubMed: 29439295]
22. Zhang F, Wei K, Slowikowski K, Fonseka CY, Rao DA, Kelly S, Goodman SM, Tabechian D, Hughes LB, Salomon-Escoto K, Watts GFM, Apruzzese W, Lieb DJ, Boyle DL, Mandelin II AM; Accelerating Medicines Partnership: RA Phase 1, AMP RA/SLE, Boyce BF, DiCarlo E, Gravallese EM, Gregersen PK, Moreland L, Firestein GS, Hacohen N, Nusbaum C, Lederer JA, Perlman H, Pitzalis C, Filer A, Holers VM, Bykerk VP, Donlin LT, Anolik JH, Brenner MB, Raychaudhuri S, Defining inflammatory cell states in rheumatoid arthritis joint synovial tissues by integrating single-cell transcriptomics and mass cytometry. Nat. Immunol 10.1038/s41590-019-0378-1 (2019).
23. Villani AC, Satija R, Reynolds G, Sarkizova S, Shekhar K, Fletcher J, Griesbeck M, Butler A, Zheng S, Lazo S, Jardine L, Dixon D, Stephenson E, Nilsson E, Grundberg I, McDonald D, Filby A, Li W, De Jager PL, Rozenblatt-Rosen O, Lane AA, Haniffa M, Regev A, Hacohen N, Single-cell RNA-seq reveals new types of human blood dendritic cells, monocytes, and progenitors. Science 356, eaah4573 (2017). [PubMed: 28428369]
24. Suram S, Silveira LJ, Mahaffey S, Brown GD, Bonventre JV, Williams DL, Gow NAR, Bratton DL, Murphy RC, Leslie CC, Cytosolic phospholipase $A_2\alpha$ and eicosanoids regulate expression of genes in macrophages involved in host defense and inflammation. PLOS ONE 8, e69002 (2013). [PubMed: 23950842]
25. Pei L, Castrillo A, Chen M, Hoffmann A, Tontonoz P, Induction of NR4A orphan nuclear receptor expression in macrophages in response to inflammatory stimuli. J. Biol. Chem 280, 29256–29262 (2005). [PubMed: 15964844]
26. Zahuczky G, Kristóf E, Majai G, Fésüs L, Differentiation and glucocorticoid regulated apopto-phagocytic gene expression patterns in human macrophages. Role of Mertk in enhanced phagocytosis. PLOS ONE 6, e21349 (2011). [PubMed: 21731712]
27. Frucht DM, Aringer M, Galon J, Danning C, Brown M, Fan S, Centola M, Wu C-Y, Yamada N, El Gabalawy H, O'Shea JJ, Stat4 is expressed in activated peripheral blood monocytes, dendritic cells, and macrophages at sites of Th1-mediated inflammation. J. Immunol 164, 4659–4664 (2000). [PubMed: 10779770]
28. Feldmann M, Translating molecular insights in autoimmunity into effective therapy. Annu. Rev. Immunol 27, 1–27 (2009). [PubMed: 19007330]
29. Remmers EF, Plenge RM, Lee AT, Graham RR, Hom G, Behrens TW, de Bakker PI, Le JM, Lee HS, Batliwalla F, Li W, Masters SL, Booty MG, Carulli JP, Padyukov L, Alfredsson L, Klareskog L, Chen WV, Amos CI, Criswell LA, Seldin MF, Kastner DL, Gregersen PK, STAT4 and the risk of rheumatoid arthritis and systemic lupus erythematosus. N. Engl. J. Med 357, 977–986 (2007). [PubMed: 17804842]
30. Gordon RA, Grigoriev G, Lee A, Kalliolias GD, Ivashkiv LB, The interferon signature and *STAT1* expression in rheumatoid arthritis synovial fluid macrophages are induced by tumor necrosis factor a and counter-regulated by the synovial fluid microenvironment. Arthritis Rheum 64, 3119–3128 (2012). [PubMed: 22614743]
31. Stephenson W, Donlin LT, Butler A, Rozo C, Bracken B, Rashidfarrokhi A, Goodman SM, Ivashkiv LB, Bykerk VP, Orange DE, Darnell RB, Swerdlow HP, Satija R, Single-cell RNA-seq of rheumatoid arthritis synovial tissue using low-cost microfluidic instrumentation. Nat. Commun 9, 791 (2018). [PubMed: 29476078]
32. Donlin LT, Jayatilleke A, Giannopoulou EG, Kalliolias GD, Ivashkiv LB, Modulation of TNF-induced macrophage polarization by synovial fibroblasts. J. Immunol 193, 2373–2383 (2014). [PubMed: 25057003]

Author Manuscript Author Manuscript Author Manuscript Author Manuscript

33. Edwards JP, Zhang X, Mosser DM, The expression of heparin-binding epidermal growth factor-like growth factor by regulatory macrophages. J. Immunol 182, 1929–1939 (2009). [PubMed: 19201846]
34. Hildenbrand R, Wolf G, Böhme B, Bleyl U, Steinborn A, Urokinase plasminogen activator receptor (CD87) expression of tumor-associated macrophages in ductal carcinoma in situ, breast cancer, and resident macrophages of normal breast tissue. J. Leukoc. Biol 66, 40–49 (1999). [PubMed: 10410988]
35. Schmidt SV, Krebs W, Ulas T, Xue J, Baßler K, Günther P, Hardt A-L, Schultze H, Sander J, Klee K, Theis H, Kraut M, Beyer M, Schultze JL, The transcriptional regulator network of human inflammatory macrophages is defined by open chromatin. Cell Res 26, 151–170 (2016). [PubMed: 26729620]
36. Wright HL, Moots RJ, Edwards SW, The multifactorial role of neutrophils in rheumatoid arthritis. Nat. Rev. Rheumatol 10, 593–601 (2014). [PubMed: 24914698]
37. Cornish AL, Campbell IK, McKenzie BS, Chatfield S, Wicks IP, G-CSF and GM-CSF as therapeutic targets in rheumatoid arthritis. Nat. Rev. Rheumatol 5, 554–559 (2009). [PubMed: 19798030]
38. Ware MF, Wells A, Lauffenburger DA, Epidermal growth factor alters fibroblast migration speed and directional persistence reciprocally and in a matrix-dependent manner. J. Cell Sci 111 (Pt 16), 2423–2432 (1998). [PubMed: 9683636]
39. Bottini N, Firestein GS, Duality of fibroblast-like synoviocytes in RA: Passive responders and imprinted aggressors. Nat. Rev. Rheumatol 9, 24–33 (2013). [PubMed: 23147896]
40. Noss EH, Brenner MB, The role and therapeutic implications of fibroblast-like synoviocytes in inflammation and cartilage erosion in rheumatoid arthritis. Immunol. Rev 223, 252–270 (2008). [PubMed: 18613841]
41. Naylor AJ, Filer A, Buckley CD, The role of stromal cells in the persistence of chronic inflammation. Clin. Exp. Immunol 171, 30–35 (2012).
42. Pap T, Müller-Ladner U, Gay RE, Gay S, Fibroblast biology. Role of synovial fibroblasts in the pathogenesis of rheumatoid arthritis. Arthritis Res 2, 361–367 (2000). [PubMed: 11094449]
43. Arnett FC, Edworthy SM, Bloch DA, McShane DJ, Fries JF, Cooper NS, Healey LA, Kaplan SR, Liang MH, Luthra HS, Medsger TA Jr., Mitchell DM, Neustadt DH, Pinals RS, Schaller JG, Sharp JT, Wilder RL, Hunder GG, The American Rheumatism Association 1987 revised criteria for the classification of rheumatoid arthritis. Arthritis Rheum 31, 315–324 (1988). [PubMed: 3358796]
44. Aletaha D, Neogi T, Silman AJ, Funovits J, Felson DT, Bingham III CO, Birnbaum NS, Burmester GR, Bykerk VP, Cohen MD, Combe B, Costenbader KH, Dougados M, Emery P, Ferraccioli G, Hazes JMW, Hobbs K, Huizinga TW, Kavanaugh A, Kay J, Kvien TK, Laing T, Mease P, Ménard HA, Moreland LW, Naden RL, Pincus T, Smolen JS, Stanislawska-Biernat E, Symmons D, Tak PP, Upchurch KS, Vencovský J, Wolfe F, Hawker G, 2010 rheumatoid arthritis classification criteria: An American College of Rheumatology/European League Against Rheumatism collaborative initiative. Arthritis Rheum 62, 2569–2581 (2010). [PubMed: 20872595]
45. Slansky E, Li J, Häupl T, Morawietz L, Krenn V, Pessler F, Quantitative determination of the diagnostic accuracy of the synovitis score and its components. Histopathology 57, 436–443 (2010). [PubMed: 20840673]
46. Orange DE, Agius P, DiCarlo EF, Robine N, Geiger H, Szymonifka J, McNamara M, Cummings R, Andersen KM, Mirza S, Figgie M, Ivashkiv LB, Pernis AB, Jiang CS, Frank MO, Darnell RB, Lingampali N, Robinson WH, Gravallese E; Accelerating Medicines Partnership in Rheumatoid Arthritis and Lupus Network, Bykerk P, Goodman SM, Donlin LT, Identification of three rheumatoid arthritis disease subtypes by machine learning integration of synovial histologic features and RNA sequencing data. Arthritis Rheumatol 70, 690–701 (2018). [PubMed: 29468833]
47. Donlin LT, Rao DA, Wei K, Slowikowski K, McGeachy MJ, Turner JD, Meednu N, Mizoguchi F, Gutierrez-Arcelus M, Lieb DJ, Keegan J, Muskat K, Hillman J, Rozo C, Ricker E, Eisenhaure TM, Li S, Browne EP, Chicoine A, Sutherby D, Noma A; Accelerating Medicines Partnership RA/SLE Network, Nusbaum C, Kelly S, Pernis AB, Ivashkiv LB, Goodman SM, Robinson WH, Utz PJ, Lederer JA, Gravallese EM, Boyce BF, Hacohen N, Pitzalis C, Gregersen PK, Firestein GS, Raychaudhuri S, Moreland LW, Holers VM, Bykerk VP, Filer A, Boyle DL, Brenner MB, Anolik

Author Manuscript Author Manuscript Author Manuscript Author Manuscript

JH, Methods for high-dimensional analysis of cells dissociated from cryopreserved synovial tissue. Arthritis Res. Ther 20, 139 (2018). [PubMed: 29996944]

48. Brennan FM, Chantry D, Jackson A, Maini R, Feldmann M, Inhibitory effect of TNF alpha antibodies on synovial cell interleukin-1 production in rheumatoid arthritis. Lancet 2, 244–247 (1989). [PubMed: 2569055]
49. Weinblatt ME, Kremer JM, Bankhurst AD, Bulpitt KJ, Fleischmann RM, Fox RI, Jackson CG, Lange M, Burge DJ, A trial of etanercept, a recombinant tumor necrosis factor receptor: Fc fusion protein, in patients with rheumatoid arthritis receiving methotrexate. N. Engl. J. Med 340, 253–259 (1999). [PubMed: 9920948]
50. Maini R, St Clair EW, Breedveld F, Furst D, Kalden J, Weisman M, Smolen J, Emery P, Harriman G, Feldmann M, Lipsky P, Infliximab (chimeric anti-tumour necrosis factor alpha monoclonal antibody) versus placebo in rheumatoid arthritis patients receiving concomitant methotrexate: A randomised phase III trial. ATTRACT Study Group. Lancet 354, 1932–1939 (1999). [PubMed: 10622295]
51. Zizzo G, Hilliard BA, Monestier M, Cohen PL, Efficient clearance of early apoptotic cells by human macrophages requires M2c polarization and MerTK induction. J. Immunol 189, 3508–3520 (2012). [PubMed: 22942426]
52. Georgoudaki AM, Prokopec KE, Boura VF, Hellqvist E, Sohn S, Ostling J, Dahan R, Harris RA, Rantalainen M, Klevebring D, Sund M, Brage SE, Fuxe J, Rolny C, Li F, Ravetch JV, Karlsson MC, Reprogramming tumor-associated macrophages by antibody targeting inhibits cancer progression and metastasis. Cell Rep 15, 2000–2011 (2016). [PubMed: 27210762]
53. da Rocha RF, De Bastiani MA, Klamt F, Bioinformatics approach to evaluate differential gene expression of M1/M2 macrophage phenotypes and antioxidant genes in atherosclerosis. Cell Biochem. Biophys 70, 831–839 (2014). [PubMed: 24771407]
54. Zelenay S, van der Veen AG, Bottcher JP, Snelgrove KJ, Rogers N, Acton SE, Chakravarty P, Girotti MR, Marais R, Quezada SA, Sahai E, Reis e Sousa C, Cyclooxygenase-dependent tumor growth through evasion of immunity. Cell 162, 1257–1270 (2015). [PubMed: 26343581]
55. Mayer-Barber KD, Andrade BB, Oland SD, Amaral EP, Barber DL, Gonzales J, Derrick SC, Shi R, Kumar NP, Wei W, Yuan X, Zhang G, Cai Y, Babu S, Catalfamo M, Salazar AM, Via LE, Barry III CE, Sher A, Host-directed therapy of tuberculosis based on interleukin-1 and type I interferon crosstalk. Nature 511, 99–103 (2014). [PubMed: 24990750]
56. Coulombe F, Jaworska J, Verway M, Tzelepis F, Massoud A, Gillard J, Wong G, Kobinger G, Xing Z, Couture C, Joubert P, Fritz JH, Powell WS, Divangahi M, Targeted prostaglandin E2 inhibition enhances antiviral immunity through induction of type I interferon and apoptosis in macrophages. Immunity 40, 554–568 (2014). [PubMed: 24726877]
57. Satoh T, Nakagawa K, Sugihara F, Kuwahara R, Ashihara M, Yamane F, Minowa Y, Fukushima K, Ebina I, Yoshioka Y, Kumanogoh A, Akira S, Identification of an atypical monocyte and committed progenitor involved in fibrosis. Nature 541, 96–101 (2017). [PubMed: 28002407]
58. Misharin AV, Morales-Nebreda L, Reyfman PA, Cuda CM, Walter JM, McQuattie-Pimentel AC, Chen C-I, Anekalla KR, Joshi N, Williams KJN, Abdala-Valencia H, Yacoub TJ, Chi M, Chiu S, Gonzalez-Gonzalez FJ, Gates K, Lam AP, Nicholson TT, Homan PJ, Soberanes S, Dominguez S, Morgan VK, Saber R, Shaffer A, Hinchcliff M, Marshall SA, Bharat A, Berdnikovs S, Bhorade SM, Bartom ET, Morimoto RI, Balch WE, Sznajder JI, Chandel NS, Mutlu GM, Jain M, Gottardi CJ, Singer BD, Ridge KM, Bagheri N, Shilatifard A, Budinger GRS, Perlman H, Monocyte-derived alveolar macrophages drive lung fibrosis and persist in the lung over the life span. J. Exp. Med 214, 2387–2404 (2017). [PubMed: 28694385]
59. Burzyn D, Kuswanto W, Kolodin D, Shadrach JL, Cerletti M, Jang Y, Sefik E, Tan TG, Wagers AJ, Benoist C, Mathis D, A special population of regulatory T cells potentiates muscle repair. Cell 155, 1282–1295 (2013). [PubMed: 24315098]
60. Issuree PD, Maretzky T, McIlwain DR, Monette S, Qing X, Lang PA, Swendeman SL, Park-Min K-H, Binder N, Kalliolias GD, Yarilina A, Horiuchi K, Ivashkiv LB, Mak TW, Salmon JE, Blobel CP, iRHOM2 is a critical pathogenic mediator of inflammatory arthritis. J. Clin. Invest 123, 928–932 (2013). [PubMed: 23348744]
61. Harada M, Kamimura D, Arima Y, Kohsaka H, Nakatsuji Y, Nishida M, Atsumi T, Meng J, Bando H, Singh R, Sabharwal L, Jiang J-J, Kumai N, Miyasaka N, Sakoda S, Yamauchi-Takihara K,

Author Manuscript Author Manuscript Author Manuscript Author Manuscript

Ogura H, Hirano T, Murakami M, Temporal expression of growth factors triggered by epiregulin regulates inflammation development. J. Immunol 194, 1039–1046 (2015). [PubMed: 25556244]

62. Swanson CD, Akama-Garren EH, Stein EA, Petralia JD, Ruiz PJ, Edalati A, Lindstrom TM, Robinson WH, Inhibition of epidermal growth factor receptor tyrosine kinase ameliorates collagen-induced arthritis. J. Immunol 188, 3513–3521 (2012). [PubMed: 22393153]
63. Gompels LL, Malik NM, Madden L, Jin P, Feldmann M, Shepard HM, Paleolog EM, Human epidermal growth factor receptor bispecific ligand trap RB200: Abrogation of collagen-induced arthritis in combination with tumour necrosis factor blockade. Arthritis Res. Ther 13, R161 (2011). [PubMed: 21982514]
64. Qing X, Chinenov Y, Redecha P, Madaio M, Roelofs JJTH, Farber G, Issuree PD, Donlin L, McLlwain DR, Mak TW, Blobel CP, Salmon JE, iRhom2 promotes lupus nephritis through TNF-α and EGFR signaling. J. Clin. Invest 128, 1397–1412 (2018). [PubMed: 29369823]
65. Bollée G, Flamant M, Schordan S, Fligny C, Rumpel E, Milon M, Schordan E, Sabaa N, Vandermeersch S, Galaup A, Rodenas A, Casal I, Sunnarborg SW, Salant DJ, Kopp JB, Threadgill DW, Quaggin SE, Dussaule J-C, Germain S, Mesnard L, Endlich K, Boucheix C, Belenfant X, Callard P, Endlich N, Tharaux P-L, Epidermal growth factor receptor promotes glomerular injury and renal failure in rapidly progressive crescentic glomerulonephritis. Nat. Med 17, 1242–1250 (2011). [PubMed: 21946538]
66. Kelly S, Humby F, Filer A, Ng N, Di Cicco M, Hands RE, Rocher V, Bombardieri M, D'Agostino MA, McInnes IB, Buckley CD, Taylor PC, Pitzalis C, Ultrasound-guided synovial biopsy: A safe, well-tolerated and reliable technique for obtaining high-quality synovial tissue from both large and small joints in early arthritis patients. Ann. Rheum. Dis 74, 611–617 (2015). [PubMed: 24336336]
67. Picelli S, Faridani OR, Björklund ÅK, Winberg G, Sagasser S, Sandberg R, Full-length RNA-seq from single cells using Smart-seq2. Nat. Protoc 9, 171–181 (2014). [PubMed: 24385147]
68. Hashimshony T, Senderovich N, Avital G, Klochendler A, de Leeuw Y, Anavy L, Gennert D, Li S, Livak KJ, Rozenblatt-Rosen O, Dor Y, Regev A, Yanai I, CEL-Seq2: Sensitive highly-multiplexed single-cell RNA-Seq. Genome Biol 17, 77 (2016). [PubMed: 27121950]
69. Dobin A, Davis CA, Schlesinger F, Drenkow J, Zaleski C, Jha S, Batut P, Chaisson M, Gingeras TR, STAR: Ultrafast universal RNA-seq aligner. Bioinformatics 29, 15–21 (2013). [PubMed: 23104886]
70. Love MI, Huber W, Anders S, Moderated estimation of fold change and dispersion for RNA-seq data with DESeq2. Genome Biol 15, 550 (2014). [PubMed: 25516281]
71. Leek JT, svaseq: Removing batch effects and other unwanted noise from sequencing data. Nucleic Acids Res 42, e161 (2014).
72. Subramanian A, Tamayo P, Mootha VK, Mukherjee S, Ebert BL, Gillette MA, Paulovich A, Pomeroy SL, Golub TR, Lander ES, Mesirov JP, Gene set enrichment analysis: A knowledge-based approach for interpreting genome-wide expression profiles. Proc. Natl. Acad. Sci. U.S.A 102, 15545–15550 (2005). [PubMed: 16199517]
73. Yarilina A, Xu K, Chan C, Ivashkiv LB, Regulation of inflammatory responses in tumor necrosis factor-activated and rheumatoid arthritis synovial macrophages by JAK inhibitors. Arthritis Rheum 64, 3856–3866 (2012). [PubMed: 22941906]
74. Conway JR, Lex A, Gehlenborg N, UpSetR: An R package for the visualization of intersecting sets and their properties. Bioinformatics 33, 2938–2940 (2017). [PubMed: 28645171]

Author Manuscript Author Manuscript Author Manuscript Author Manuscript

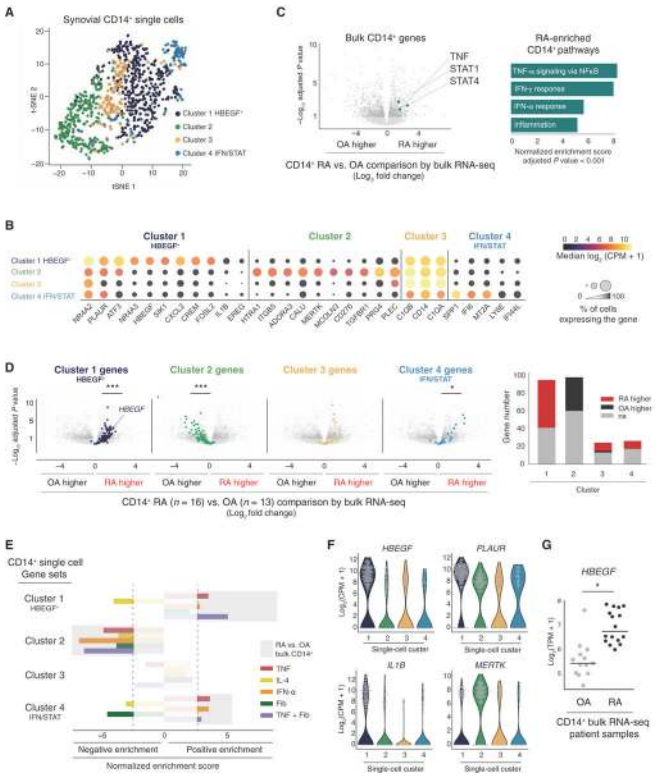

Fig. 1. HBEGF$^+$ inflammatory macrophages in RA joints identified by scRNA-seq.

(**A**) Human synovial CD14$^+$ single-cell clusters (940 cells). CD45$^+$CD14$^+$ cells were flow-sorted from synovial tissue of patients with RA ($n = 10$) or OA ($n = 2$) and processed by plate-based scRNA-seq. (**B**) CD14$^+$ single-cell cluster marker genes. Median expression of a gene across all cells in cluster is indicated by color and the percentage of cells expressing the gene in each cluster is indicated by size. (**C**) Differential gene expression of bulk CD14$^+$ synovial cell populations from patients with RA ($n = 16$) versus OA ($n = 13$) plotted as $\log_2$ fold change with $-\log_{10}$ FDR adjusted P value; dark gray <0.1. Right: Positively enriched pathways in RA bulk CD14$^+$ cells. (**D**) CD14$^+$ single-cell cluster marker genes highlighted on the bulk RA versus OA plot from (C) (up to 100 genes shown per cluster, Bonferroni-corrected $P < 0.1$, expressed in ≥30% of cells). Hypergeometric test: $^{***}P < 10^{-6}$, $^{*}P < 10^{-3}$. Right: Number of cluster genes higher in RA or OA bulk comparison or not significant (ns) (FDR adjusted $P < 0.1$). (**E**) GSEA using the CD14$^+$ single-cell markers as gene sets and ranked gene lists from human blood–derived macrophages exposed to various stimuli (colored bars) or the bulk CD14$^+$ RA versus OA analysis (background: gray bars). |NES| (normalized enrichment scores) > 2.5 were significant at FDR adjusted $P < 0.001$. (**F**) Gene expression for each CD14$^+$ single cell plotted as $\log_2$ counts per million (CPM) + 1. (**G**) *HBEGF* expression in CD14$^+$ bulk cell populations from individual patients, plotted as $\log_2$ transcripts per million (TPM) + 1. $n = 16$ RA and $n = 13$ OA samples. *Bonferroni-corrected $P < 10^{-3}$.

Author Manuscript Author Manuscript Author Manuscript Author Manuscript

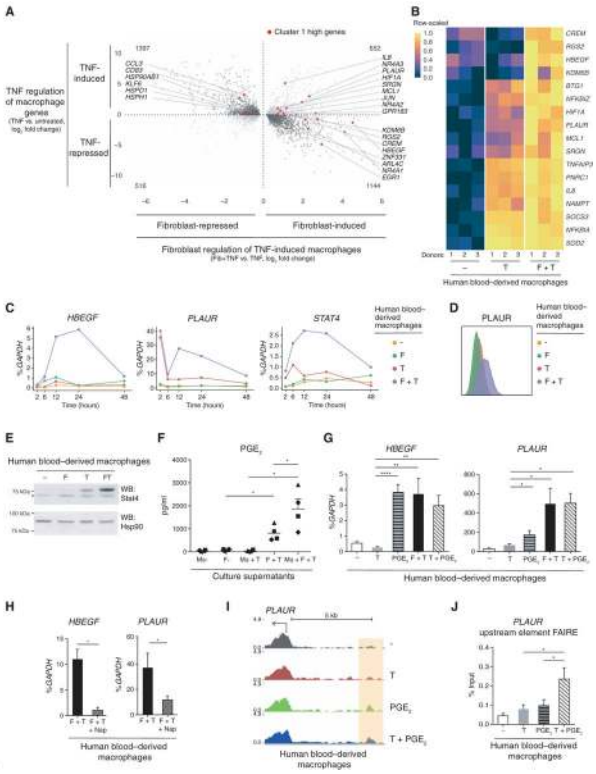

Fig. 2. HBEGF^{+} inflammatory macrophage polarization by tissue fibroblasts.

(**A**) Human blood–derived macrophage genes regulated by synovial fibroblasts and TNF (3709 genes, FDR adjusted $P < 0.1$; $n = 4$ donors). Expression changes plotted as $\log_2$ fold. The *x*-axis plots fibroblasts + TNF versus TNF; the *y* axis plots TNF versus untreated. HBEGF^{+} cluster 1 single-cell markers labeled in red (expressed in >55% of cells, Bonferroni-corrected $P < 10^{-6}$). (**B**) Expression of select synovial CD14^{+} cluster 1 genes in the blood-derived macrophages exposed to TNF (T) or fibroblasts + TNF (F + T). $n = 3$ donors. (**C**) qPCR of blood-derived macrophage gene expression over time, plotted as percentage (%) of *GAPDH* (glyceraldehyde-3-phosphate dehydrogenase). Representative of $n = 4$ donors. (**D**) The PLAUR gene cell surface protein product (CD87) detected by flow cytometry in blood-derived macrophage cultures at 24 hours. (**E**) Western blot of STAT4 in blood-derived macrophage cultures at 24 hours. Representative of $n = 4$ donors. Asterisk (*) denotes nonspecific band. Hsp90, loading control. (**F**) PGE_2 enzyme-linked immunosorbent assay (ELISA) using supernatants from blood-derived macrophage (Mϕ) cultures at 24 hours. $n = 4$ donors. Data are means ± SEM. (**G**) qPCR of blood-derived macrophage gene expression in cultures at 24 hours. $n = 8$ donors. (**H**) qPCR of blood-derived macrophage gene expression in culture at 24 hours. Nap, COX inhibitor naproxen (150 nM). (**I**) ATAC-seq tracks from *PLAUR* gene promoter regions in blood-derived macrophage cultures at 3 hours. The region with light orange highlight is further examined in (J). The arrow indicates transcription start site. (**J**) FAIRE-qPCR analysis of open chromatin for the region highlighted in (I), % total input reported as mean ± SEM. $n = 4$ donors. $^{*}P < 0.05$, $^{**}P < 0.01$, and $^{****}P < 0.0001$.

Author Manuscript Author Manuscript Author Manuscript Author Manuscript

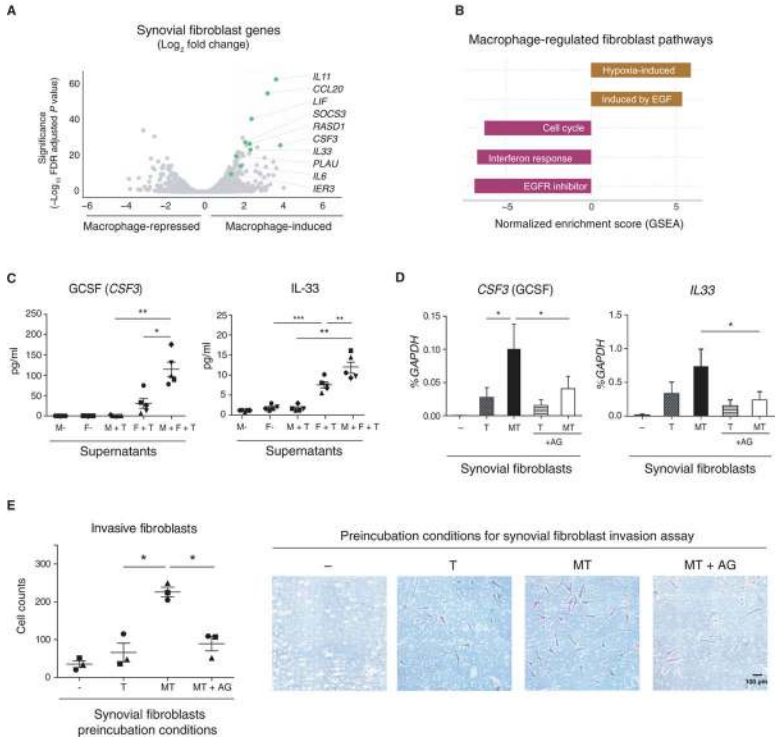

Fig. 3. HBEGF^{+} inflammatory macrophages promote EGFR-dependent synovial fibroblast pathologic activity.

(**A**) Human synovial fibroblast genes altered by blood-derived macrophages during a TNF response (885 genes differentially expressed), RNA-seq, 48 hours. $n = 2$ donors. x axis: $\log_2$ fold change by macrophages. y axis: significance as the $-\log_{10}$ FDR adjusted P value. (**B**) Fibroblast pathways regulated by macrophages under TNF conditions (GSEA and IPA). Macrophage-induced, brown. Macrophage–down-regulated, maroon. (**C**) ELISA assay using supernatants of synovial fibroblast (F) cultures with or without macrophages (M) and TNF (T) for 48 hours. $n = 4$ donors for both, reported as mean with SEM. (**D**) qPCR on fibroblast cultures at 32 hours. EGF receptor inhibitor, AG 1478 (AG, 4 μM). Mean ± SEM. $n = 6$ donors. (**E**) Cell counts and photomicrographs of synovial fibroblast Matrigel invasion assay with crystal violet stain, 18 hours after a 24-hour preincubation with macrophages (M), TNF (T), and the EGFR inhibitor (AG). $n = 3$ donors. $^{*}P < 0.05$, $^{**}P < 0.01$, and $^{***}P < 0.001$ by paired Student's t test, respectively.

Author Manuscript Author Manuscript Author Manuscript Author Manuscript

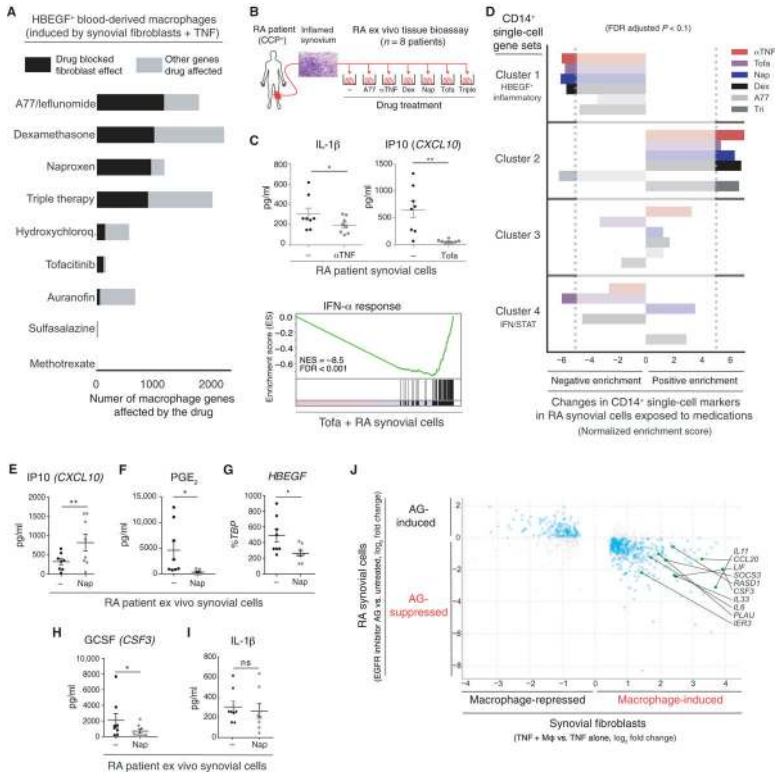

Fig. 4. Clinically effective RA medications and a therapeutic EGFR inhibitor target HBEGF$^+$ inflammatory macrophage-fibroblast cross-talk in RA tissue.

(**A**) Number of blood-derived macrophage genes affected by RA medications in the presence of TNF and synovial fibroblasts from cultures at 24 hours. Black, fibroblast-regulated genes opposed by drug. Gray, all other genes regulated by drug. FDR adjusted $P < 0.1$. $n = 2$ to 4 donors. (**B**) RA patient synovial tissue ex vivo drug response assay using highly inflamed synovium (scored by histology) from patients with positive blood titers for anti–cyclic citrullinated peptide (CCP$^+$) antibodies. Dissociated cells placed into culture were exposed to a panel of medications for 24 hours. αTNF, anti-TNF antibodies. (**C**) ELISA using supernatants from RA tissue ex vivo assay. $n = 8$ donors. *$P < 0.05$ and **$P < 0.01$ by Wilcoxon signed-rank test. Bottom: IFN-α response upon tofacitinib exposure, bulk RNA-seq, and GSEA. $n = 2$ donors. (**D**) Direction and intensity of change for CD14$^+$ single-cell cluster markers in RA synovial cells exposed to various medications. Normalized enrichment scores (GSEA). (**E**, **H**, and **I**) ELISAs as described in (C). (**F**) PGE_2 ELISA using supernatants. Data are means ± SEM. $n = 7$ donors. *$P < 0.05$, paired Student's t test. (**G**) qPCR using ex vivo synovial cells treated with naproxen, plotted as percentage (%) of TBP. $n = 7$ donors. Data are means ± SEM. *$P < 0.05$, paired Student's t test. (**J**) Gene expression changes induced by the EGFR inhibitor AG-1478 in RA patient ex vivo synovial cells (y axis) compared to changes in synovial fibroblasts induced by macrophages and TNF (x axis, data from Fig. 3A); $n = 2$ donors. FDR adjusted $P < 0.1$, plotted as a $\log_2$ fold change. Highlighted genes are from Fig. 3A.